



HAL
open science

Modelling energy deposition in TR image plate detectors for various ion types

V. Lelasseux, J. Fuchs

► **To cite this version:**

V. Lelasseux, J. Fuchs. Modelling energy deposition in TR image plate detectors for various ion types. *Journal of Instrumentation*, 2020, 15 (04), pp.P04002-P04002. 10.1088/1748-0221/15/04/P04002 . hal-02566056

HAL Id: hal-02566056

<https://hal.science/hal-02566056v1>

Submitted on 12 Nov 2020

HAL is a multi-disciplinary open access archive for the deposit and dissemination of scientific research documents, whether they are published or not. The documents may come from teaching and research institutions in France or abroad, or from public or private research centers.

L'archive ouverte pluridisciplinaire **HAL**, est destinée au dépôt et à la diffusion de documents scientifiques de niveau recherche, publiés ou non, émanant des établissements d'enseignement et de recherche français ou étrangers, des laboratoires publics ou privés.

OPEN ACCESS

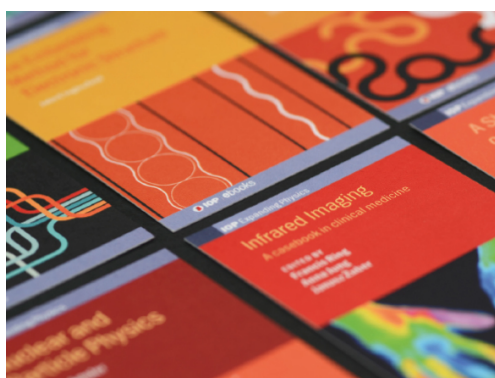
Modelling energy deposition in TR image plate detectors for various ion types

To cite this article: V. Lelasseux and J. Fuchs 2020 *JINST* **15** P04002

View the [article online](#) for updates and enhancements.

Recent citations

- [Ion species discrimination method by linear energy transfer measurement in Fujifilm BAS-SR imaging plate](#)
M. Nishiuchi *et al*



IOP | ebooks™

Bringing together innovative digital publishing with leading authors from the global scientific community.

Start exploring the collection—download the first chapter of every title for free.

Modelling energy deposition in TR image plate detectors for various ion types

V. Lelasseux¹ and J. Fuchs

LULI — CNRS, CEA, UPMC Univ Paris 06: Sorbonne Université,
Ecole Polytechnique, Institut Polytechnique de Paris,
F-91128 Palaiseau cedex, France

E-mail: vincent.lelasseux@polytechnique.edu, julien.fuchs@polytechnique.edu

ABSTRACT: This paper presents an empirical model for the response of Fuji BAS-TR image plate (IP) for various type of energetic ions. This model has been obtained using the works of Bonnet et al. [*Rev. Sci. Instrum.* **84** (2013) 103510] and Birks [*Proc. Phys. Soc. A* **64** (1951) 874] and has been confronted to several experimental sets of data, showing its validity and its limits for high Z ions.

KEYWORDS: Detector modelling and simulations I (interaction of radiation with matter, interaction of photons with matter, interaction of hadrons with matter, etc); Solid state detectors

¹Corresponding author.

Contents

1	Introduction	1
2	Background and rationale for the empirical approach	1
3	Results	2
4	Conclusion	6

1 Introduction

Several types of detectors [1] exist in order to diagnose energetic ions. Solid state detectors such as CR-39, radiochromic films (RCF), scintillators or image plates (IP) [2], belong to one type. Passiveness and immunity to electromagnetic pulses are particularly interesting features of such detectors. Among these solid state detectors, IPs use phosphorescent properties to store energy left by energetic particles going through them. Then, this energy can be retrieved with scanners which will stimulate the induced metastable excited states, using photons with a suitable wavelength. Those devices developed by Fujifilm in the early 1980's have since been quite popular in medicine and physics due to some of their useful features. Indeed, IP can be reused after a 15 min erasing sequence induced by an intense visible light source. Besides, an IP has a high dynamic range (up to 5 order of magnitude) and a very good spatial resolution (down to 10 μm) usually limited by the scanner properties [2]. This dynamic range can even be enhanced using advanced scanning techniques [3].

At the end of the scanning process, the result is an image of quantum levels (QL) which can then be used to calculate photostimulated luminescence (PSL) values which is a function of the incident particles energy [4]. However, there is still no theoretical formula to get the relation between PSL and the energy incident in the detector for any type of ion. Then, a calibration is needed if one wants to retrieve quantitative data from the recorded PSL [2, 5–9]. In order to avoid such time-consuming calibrations, this paper will try to find an empirical formula for this problem using Bonnet work [5] and Birks' formula [10]. Besides, this work will use calibration datasets [2, 5–9, 11, 12] from previous experiments to gauge the adequacy of the method. We will here focus on one type of IPs in particular, the BAS TR ones from Fuji, which main composition is detailed in table 1 [6].

2 Background and rationale for the empirical approach

Between the IPs irradiation and their scanning, there is always a time lag, allowing for some recombinations to happen. As a consequence, the detectable signal is a time-dependent function

Table 1. The BAS TR IPs are composed of three different layers as show in this table [2, 6].

Layer	Width (μm)	Composition	Density ($\text{g}\cdot\text{cm}^{-3}$)
Phosphor	50	BaFBr _{0.85} I _{0.15}	2.85
Support	250	C ₂ H ₂ O	1.66
Magnetic	160	ZnMn ₂ Fe ₅ NO ₄₀ H ₁₅ C ₁₀	2.77

which is characterized by the fading of the signal in the IP [6]. Bonnet finds that the original signal must be multiplied by the following function to get the detectable signal [6]:

$$f(t) = \sum_{i=1}^2 B_i e^{-\frac{t}{\beta_i}} \quad (2.1)$$

Those parameters do not seem to depend on the ion type nor their incident energy. However, those parameters depend on the temperature and the scanner used. Using the FLA-7000 scanner at ambient temperature and IPs irradiated by protons of 1.5 MeV, Bonnet finds for the protons:

$$B_1 = 0.49, \quad \beta_1 = 17.9 \text{ min}, \quad B_2 = 0.51, \quad \beta_2 = 1482 \text{ min}$$

According to Bonnet [5], after multiplying by the fading factor, the IP response is given by:

$$R(E) = A_i \int_0^W \frac{dE_{\text{dep}}}{dz}(E, z) e^{-\frac{z}{L}} dz \quad (2.2)$$

where $R(E)$ is the PSL signal for a proton with an initial energy E , W the width of the active layer, E_{dep} the deposited energy, A_i a parameter a priori depending on the ion and the IP type and L is the absorption length of the scanning photons (2–3 eV).

In order to remove the dependence of eq. (2.2) on a particular ion, we can use the work of Birks [10] that models the specific fluorescence of an organic crystal following its irradiation. Adapting it to model the response of the IP would yield the following empirical formula, independent from the ion:

$$R(E) = \sum_i A \int_{C_i} \frac{\frac{dE_{\text{dep}}}{dz}(E, z)}{1 + B \left| \frac{dE_{\text{dep}}}{dz} \right|} e^{-\frac{z}{L}} dz \quad (2.3)$$

where $R(E)$ is the PSL signal, A a parameter only dependent of the IP, L is the absorption length of the scanning photons (2–3 eV), C_i the route of one ion and B a saturation coefficient.

3 Results

We will now attempt to confront eq. (2.3) to measured calibration data. Using SRIM [13], a compilation of large experimental datasets related to ion energy deposition in matter, it is possible to get the energy deposited as a function of depth (dE/dz), for any ion type and any energy. As shown in table 1, the TR IPs are characterized by a 50 μm thick sensitive layer with the composition BaFBr_{0.85}I_{0.15} [6]. From those deposited energies, we can use the following function to calculate a PSL quantity:

$$R(E) = A \int_0^W \frac{\frac{dE_{\text{dep}}}{dz}(E, z)}{1 + B \left| \frac{dE_{\text{dep}}}{dz} \right|} e^{-\frac{z}{L}} dz \quad (3.1)$$

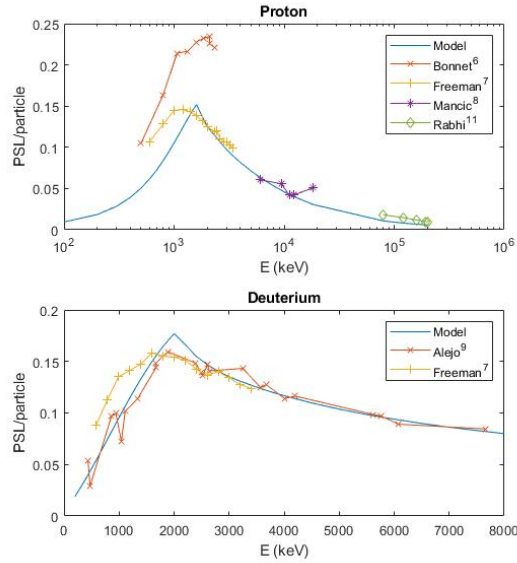


Figure 1. The panels show the PSL response of the TR image plate as measured experimentally by various groups or calculated (see text). For the calculations, the model uses $A = 3.0 \times 10^{-4}$ PSL.keV $^{-1}$ and $B = 0.15$ $\mu\text{m}.\text{eV}^{-1}$.

From the work of Bonnet [6], we get that $L = 44$ μm . Using datasets from Bonnet et al. [5, 6], Freeman et al. [7], Mancic et al. [8], Doria et al. [2], Alejo et al. [9] and Rabhi et al. [11], we have been able to find parameters for which this model fits pretty well these experimental data. The results for $A = 3.0 \times 10^{-4}$ PSL.keV $^{-1}$ and $B = 0.15$ $\mu\text{m}.\text{eV}^{-1}$ are shown in figure 1 and figure 2.

Aside from the proton calibration data of Bonnet [6], which are not in total agreement with the Freeman dataset [7], we observe in figure 1 and figure 2 that the model of eq. (3.1) corresponds quite well to the measured calibrations of the TR IP for proton, deuterium, alpha and carbon ions. The recent work of Strehlow [12] giving calibration data relative to Ti ions, allows to check extending the validity of eq. (3.1) to heavier ions. In this case, as evidenced by figure 3, there is however a significant departure between the model and the data.

Trying to find parameters, which could fit all the data for the light and heavy ions simultaneously, results in a mediocre compromise as shown in figure 4, figure 5 and figure 6. Indeed, we see on those figures that although a good fit can be obtained for the Ti data, this set of parameters underestimates the PSL calibration for very light nuclei (proton and deuterium) and overestimates it for light nuclei (alpha and carbon).

One could wonder about the influence of a component of the phosphor layer which we neglected till now. Indeed, the BaFBr $_{0.85}$ I $_{0.15}$ crystals are embedded in a urethane resin. It's hard to find the precise mixture of the crystal and the resin but using the BAS-MS composition [14] and the density of the MS and TR IP's phosphor layer, we can estimate a 8:1 BaFBr $_{0.85}$ I $_{0.15}$:urethane mix. Besides, it's not possible in SRIM to get the different energy deposited in those two different part of the mix. More complicated Geant4 simulations would then be needed to get more precise results. However, as it can be seen on figure 7 with proton and Ti ions, the total energy deposition doesn't change that much when taking or not into account the resin in the mixture. Thus, the presence of the resin is

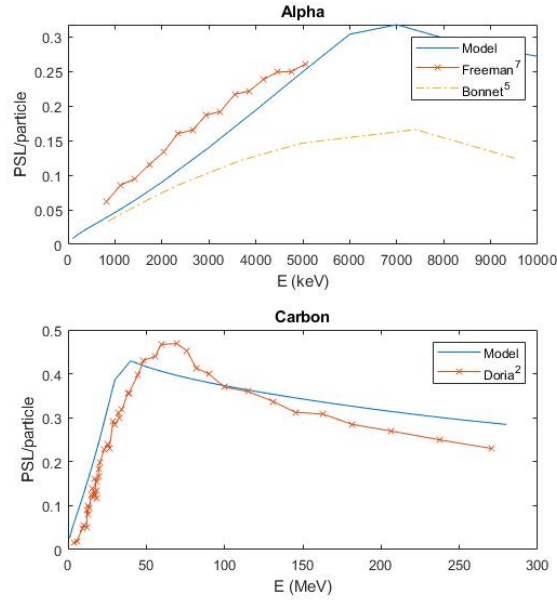


Figure 2. The panels show the PSL response, per incident ion, of the TR image plate as measured experimentally by various groups or calculated (see text). For the calculations, the model uses $A = 3.0 \times 10^{-4} \text{ PSL.keV}^{-1}$ and $B = 0.15 \text{ }\mu\text{m.eV}^{-1}$.

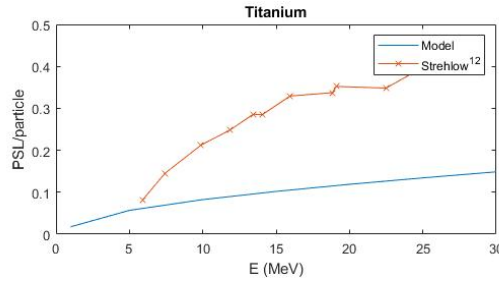


Figure 3. PSL response of TR image plate for Ti measured experimentally and calculated for $A = 3.0 \times 10^{-4} \text{ PSL.keV}^{-1}$ and $B = 0.15 \text{ }\mu\text{m.eV}^{-1}$.

not the factor that can explain the inability of the model to fit both the light and heavy ions energy deposition.

Besides, as can be observed from the case of the carbon curve of figure 2 and for titanium in figure 6, it seems that the PSL response for low energies are always overestimated even if when the fit seems nice. As a consequence, we can wonder if, in general, the models which links deposited energy with the PSL response are still totally accurate for nuclei heavier than helium. Indeed, Doria's data [2] seems to show that the energy where the PSL response is maximum is higher than the one modelled as can be seen in figure 2. One important aspect of the present modeling is that we assumed that there is a one-to-one relation between the energy deposited by the ion in the IP, which is well-known, and the energy stored in the Eu ions metastable states. The difficulty we observe in fitting the model with the data would suggest that the energy transferred by heavy ions to the excited Eu ions in the IP takes other, more efficient, channels than when the energy deposited is low, as for light ions.

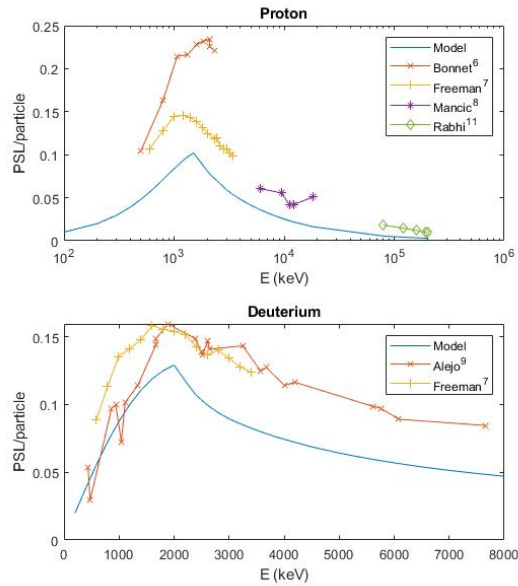


Figure 4. The panels show the PSL response of the TR image plate as measured experimentally by various groups or calculated (see text). For the calculations, the model uses $A = 1.5 \times 10^{-4}$ PSL.keV $^{-1}$ and $B = 0.02 \mu\text{m.eV}^{-1}$.

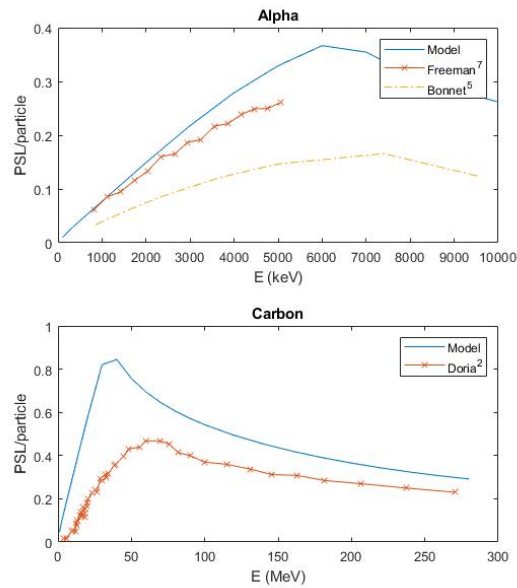


Figure 5. The panels show the PSL response of the TR image plate as measured experimentally by various groups or calculated (see text). For the calculations, the model uses $A = 1.5 \times 10^{-4}$ PSL.keV $^{-1}$ and $B = 0.02 \mu\text{m.eV}^{-1}$.

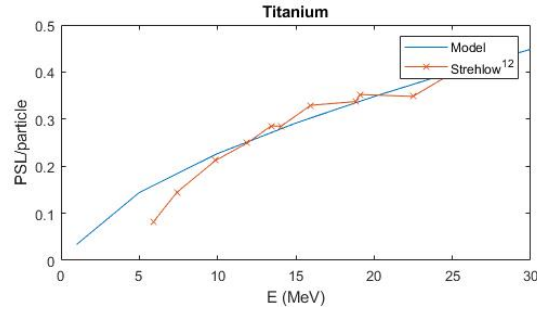


Figure 6. PSL response of TR image plate for Ti ions measured experimentally and calculated for $A = 1.5 \times 10^{-4}$ PSL.keV $^{-1}$ and $B = 0.02$ $\mu\text{m.eV}^{-1}$.

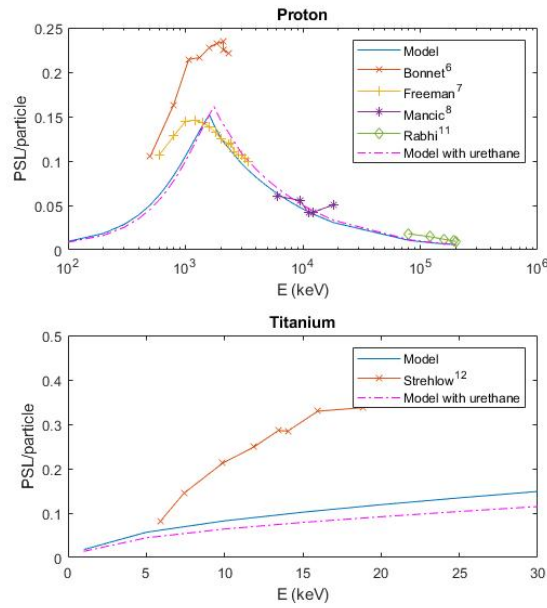


Figure 7. PSL response of TR image plate for protons and Ti ions measured experimentally and calculated for $A = 3.0 \times 10^{-4}$ PSL.keV $^{-1}$ and $B = 0.15$ $\mu\text{m.eV}^{-1}$ and composition with and without urethane resin.

4 Conclusion

Using Birks' formula [10] and Bonnet's work [6], we found an empirical formula to estimate the calibration for a type of image plate, the BAS-TR one. Hence, the requisite calibration in order to get quantitative results using image plates can now be avoided for ions with a low Z (e.g. Li). Nevertheless, it seems that this formula doesn't work with higher Z . Obviously, further investigations are needed to understand the process by which energy is stored in image plates for higher Z ions, especially at energies around where the deposited energy is maximal, to check if the link between PSL and deposited energy needs to be modified.

Acknowledgments

We acknowledge fruitful discussions with D. Doria (ELI-NP).

This project has received funding from the European Union's Horizon 2020 research and innovation program under grant agreement no 654148 Laserlab-Europe and from the European Research Council (ERC) (grant agreement No 787539). It was also supported by Grant ANR-17-CE30-0026-Pinnacle from Agence Nationale de la Recherche.

References

- [1] P. Bolton, et al., *Instrumentation for diagnostics and control of laser-accelerated proton (ion) beams*, *Phys. Med.* **30** (2014) 255 .
- [2] D. Doria et al., *Calibration of BAS-TR image plate response to high energy (3–300 MeV) carbon ions*, *Rev. Sci. Instrum.* **86** (2015) 123302.
- [3] M. Thoms, *The dynamic range of X-ray imaging with image plates*, *Nucl. Instrum. Meth. A* **389** (1997) 437.
- [4] S. Tosaki et al., *Evaluation of laser-driven ion energies for fusion fast-ignition research*, *Prog. Theor. Exp. Phys.* **2017** (2017) 103J01.
- [5] T. Bonnet et al., *Response functions of imaging plates to photons, electrons and ^4He particles*, *Rev. Sci. Instrum.* **84** (2013) 103510.
- [6] T. Bonnet et al., *Response functions of Fuji imaging plates to monoenergetic protons in the energy range 0.6–3.2 MeV*, *Rev. Sci. Instrum.* **84** (2013) 013508.
- [7] C. G. Freeman et al., *Calibration of a Thomson parabola ion spectrometer and Fujifilm imaging plate detectors for protons, deuterons, and alpha particles*, *Rev. Sci. Instrum.* **82** (2011) 073301.
- [8] A. Mančić et al., *Absolute calibration of photostimulable image plate detectors used as (0.5–20 MeV) high-energy proton detectors*, *Rev. Sci. Instrum.* **79** (2008) 073301.
- [9] A. Alejo et al., *Characterisation of deuterium spectra from laser driven multi-species sources by employing differentially filtered image plate detectors in Thomson spectrometers*, *Rev. Sci. Instrum.* **85** (2014) 093303 [[arXiv:1408.2978](https://arxiv.org/abs/1408.2978)].
- [10] J.B. Birks, *Scintillations from organic crystals: specific fluorescence and relative response to different radiations*, *Proc. Phys. Soc. A* **64** (1951) 874.
- [11] N. Rabhi et al., *Calibration of imaging plate detectors to mono-energetic protons in the range 1–200 MeV*, *Rev. Sci. Instrum.* **88** (2017) 113301.
- [12] J. Strehlow et al., *The response function of Fujifilm BAS-TR imaging plates to laser-accelerated titanium ions*, *Rev. Sci. Instrum.* **90** (2019) 083302.
- [13] M.D. Z. J.F. Ziegler and J.P. Biersack, *SRIM: the stopping and range of ions in matter*, Cadence Design Systems, 2008.
- [14] M. Stoeckl and A.A. Solodov, *Readout models for BaFBr_{0.85}I_{0.15}:Eu image plates*, *Rev. Sci. Instrum.* **89** (2018) 063101.